Relationship Between Structure and Rheological, Mechanical and Thermal Properties of Polylactide/Cloisite 30B Nanocomposites

Lynda Zaidi,[1] Stéphane Bruzaud,[2] Alain Bourmaud,[2] Pascal Médéric,[3] Mustapha Kaci,[1] Yves Grohens[2]

[1]*Laboratoire des Matériaux Organiques, Faculté de la Technologie, Université Abderrahmane Mira, Bejaia 06000, Algeria*
[2]*Laboratoire d'Ingénierie des Matériaux de Bretagne, Equipe E2PIC, Université de Bretagne Sud, Rue de Saint Maudé, Lorient Cedex 56321, France*
[3]*Laboratoire d'Ingénierie des Matériaux de Bretagne, Equipe Rhéologie, Université de Bretagne Occidentale, 6 Avenue le Gorgeu, Brest Cedex 3 29238, France*

Received 25 August 2009; accepted 21 October 2009
DOI 10.1002/app.31655
Published online 23 December 2009 in Wiley InterScience (www.interscience.wiley.com).

ABSTRACT: Melt-state and solid state mechanical properties and thermal stability of polylactide layered silicate nanocomposites elaborated by melt intercalation were studied as a function of clay content. Wide angle X-ray scattering results, transmission electron microscopy observations, and rheological measurements indicated that the clay was finely distributed in the polylactide matrix. Contrary to nonlinear mechanical properties, thermal and linear mechanical properties were shown to increase with increasing clay fraction. The nanoindentation measurements confirm the significant increase of linear mechanical properties previously observed by tensile tests. The good correlation of linear mechanical properties at the macrometric and nanometric scales is explained by the high dispersion degree of the nanofiller in the biodegradable polymer matrix. © 2009 Wiley Periodicals, Inc. J Appl Polym Sci 116: 1357–1365, 2010

Key words: polylactide; clay; nanocomposites; exfoliation

INTRODUCTION

During the last decade, significant attention has been focused on both biodegradable polymers and polymer layered silicate nanocomposites. The introduction of nanofillers in biodegradable matrices has allowed improving the range of properties and possible uses of these environmental friendly polymers.[1–3] Among all these polymers, polylactide (PLA) is one of the biodegradable polymers that can be used as promising alternative to the petroleum-based commodity materials, because they can be derived from renewable resources, such as corn, potato, and other agricultural products.[4,5] PLA is linear aliphatic thermoplastic polyester with excellent properties comparable to many petroleum-based plastics. High molecular weight PLA is generally produced by the ring-opening polymerization of lactide. Lactide is a cyclic dimer prepared by controlled depolymerization of lactic acid, which in turn is obtained from the fermentation of sugar feedstocks, corn, etc.[6,7] Moreover, PLA has good mechanical properties, thermal plasticity, high degree of transparency and biocompatibility, therefore PLA holds tremendous promise for various end-use applications such as biomedical fields, household, engineering, packaging industries.[8–10] However, some of its properties, like flexural properties, gas permeability and heat distortion temperature, are too low for widespread applications. Therefore, many attempts were carried out to reach exfoliation state in corresponding nano-biocomposites.[2] The preparation of nano-biocomposites defined as a combination between a biopolymer and an inorganic nanofiller is a route to enhance some of the biodegradable polymers properties. Nanoclays such as montmorillonite or hectorite are classically used to improve biodegradable polymers stress and stiffness, reduce their gas/water vapor barrier properties, increase their thermal stability and modify their biodegradation rate.[11,12]

Krikorian and Pochan[13] successfully prepared exfoliated materials based on PLA with randomly distributed clay platelets via solvent intercalation in the presence of Cloisite 30B (C30B). Since C30B bears a long alkyl chain and hydroxyl groups, the interactions between OH functions from the clay organomodifier and C=O moieties of the PLA backbone

Correspondence to: S. Bruzaud (stephane.bruzaud@univ-ubs.fr).
Contract grant sponsors: EGIDE, TASSILI program.

favored exfoliation. The elaboration of PLA/clay nano-biocomposites by melt intercalation is also widely described in the literature, leading to various material structures.[14–16] Okamoto and his group at Toyota Technological Institute (Nagoya, Japan) tested a lot of PLA-based systems differing from the organically modified layered silicate in the aspect ratio of the inorganic platelets, the nature of the organomodifier and the clay content.[17] Depending on these parameters, intercalated, intercalated-and-flocculated, intercalated-and-exfoliated or nearly exfoliated structures were obtained.

We have previously shown that significant layered nanofiller dispersion into several polymer matrices can be successfully accomplished using *in situ* polymerization method,[18–22] solution process,[23] or melt intercalation technique.[24,25] In this work, PLA layered silicate nanocomposites were prepared using a melt intercalation process.

Among various macroscopic material properties, melt-state rheological properties of layered silicate nanocomposites have attracted significant attention, as reviewed by Krishnamoorti and Yurekli,[26] because of their scientific interest regarding the study of structure/behavior relations and because of their technological interest regarding processability. Most experimental studies on linear viscoelastic behavior of various silicate nanocomposites show the existence of a transition from liquid-like behavior to solid-like behavior at a low silicate mass fraction usually ranging from 2 to 4 wt %.[27] The detailed study of melt rheological properties has highlighted the solid-like behavior of nanocomposites based on PLA and filled from 3 wt % of organically modified montmorillonite.[28] This property has been attributed to the formation of a "spatially-linked structure", because of the large aspect ratio of silicate particles.

In the last years, many authors have used nanoindentation to study mechanical properties of nanocomposites. Nanoindentation is a powerful tool, which can provide local properties in comparison to classical tensile test. Recently, Shen and coworkers[29] have shown that injection-molded specimens of polyamide 6 nanocomposites have higher hardness and modulus in core than in the outer part. Lam et al.[30] have investigated the elastic modulus of nanoclay-epoxy composite samples made under different sonification temperatures. They noticed a decrease of the modulus from bottom surface to the top surface of the composite because of the gravitational effect of the nanoclay clusters. Indentations performed on maleic anhydride modified polypropylene-organoclay nanocomposites have shown an important increase of hardness and modulus in clay congregated region in comparison to unreinforced region or clay-matrix boundary.[31] Mechanical properties of poly(methylmethacrylate)-SiO_2 thin films have been studied using nanoindentation technique.[32] An improvement in modulus and hardness has been observed with the increase of the indentation depth, in good agreement with the composition of the layers. Last, we have shown a significant improvement into modulus and hardness with the increase of clay loading because of the addition of stiff clay nanofillers into the poly(3-hydroxybutyrate-*co*-3-hydroxyvalerate) matrix.[23] This work has also pointed out the good agreement between the mechanical measurements carried out using tensile tests which can be considered as a macroscopic characterization technique, and those obtained by the nanoindentation technique which allows the determination of the mechanical properties at the nanometric scale. This good correlation of mechanical properties at the macrometric and nanometric scales has been attributed to a high dispersion degree of nanoplatelets within the polymer matrix.

The aim of this article is to study structure–local and macroscopic properties relationship for PLA-clay nano-biocomposite elaborated by melt intercalation. Thermal, rheological, and mechanical properties were studied as a function of clay content and discussed in terms of clay dispersion.

EXPERIMENTAL

Materials

Polylactide, in the form of pellets, was supplied by Biomer under the trade name Biomer L9000® and used as received with a D-lactide content of 4.3%. The material has a density equal to 1.25 g cm^{-3} at 23°C, an average molecular weight $\overline{M}_n$ = 220,000 g mol^{-1} and a Newtonian viscosity of about 870 Pa s at 190°C. PLA is a semicrystalline polymer with a glass transition temperature (T_g) of about 60°C and a melting temperature (T_m) of about 160°C. PLA was dried under vacuum at 60°C before use.

Cloisite 30B is an organically modified montmorillonite which is commercially available and was supplied by Southern Clay Products (Texas). C30B is a montmorillonite modified with bis-(2-hydroxyethyl) methyl tallowalkyl ammonium cations. C30B was dried under vacuum at 60°C for at least 24 h before use.

Preparation of PLA-Cloisite 30B nanocomposites

The PLA-Cloisite 30B nanocomposites were prepared by melt mixing in a Brabender Plasticorder mixer (model W 50 EHT) having the following characteristics: chamber volume of 55 cm^3, sample weight of 40–70 g, maximum torque of 200 N m and maximum temperature equal to 500°C. The major processing parameters were mixing temperature, screw speed and residence time; they were set at 190°C, 60 rpm

and 8 min, respectively. The resulting material was granulated, and then compressed to produce thin films of an average thickness of about 150 μm, using a hydraulic press equipped with two heated plates at 190°C with a pressure of 30 bars for 3 min. Different formulations based on PLA were prepared with various clay contents: 1, 3, and 5 wt %.

The degree of cristallinity of the samples was calculated from the curves obtained by differential scanning calorimetry. The average degree of cristallinity value of PLA nanocomposites was 40 ± 5% and no modification was observed with the C30B content.

As far as the nanoindentation technique is concerned, sample preparation is very important because accurate results are obtained only if the indentations are significantly deeper than the surface topography of the specimen. A meticulous polishing can significantly reduce the uncertainty in determining the surface properties. Hence, all surfaces to be indented were polished to a 3-μm particle size polishing solution finish. The average surface roughness, R_a, was measured with a profilometer at 0.3 μm. The polished samples were mounted on aluminum cylinders using Super Glue™ for subsequent indentation tests.

Characterization methods of PLA-Cloisite 30B nanocomposites

Wide angle X-ray scattering (WAXS)

WAXS was used to analyze the structure of the materials and to determine the interlayer spacing between stacked clay platelets. WAXS experiments were performed by using a Philips diffractometer (PW 1050) operating at the CuKα radiation (wavelength, λ = 0.154 nm), 40 kV, and 20 mA. The diffraction spectra were recorded in the reflection mode over a 2Θ range of 3–12° at room temperature and a scan rate of $0.017°s^{-1}$.

Transmission electron microscopy (TEM)

The different samples observed in TEM were dehydrated in ethanol solutions (up to 100%), then in 50% epon and finally 100% epon. After polymerization, the blocks are sectioned and the ultrathin sections were observed in a Philips CM12 microscope operating at 120 kV.

Rheology

Oscillatory shear measurements were performed using a controlled stress rheometer (GEMINI from Malvern Instruments) equipped with parallel disk of 25 mm. All samples were characterized at 190°C and all measurements were carried out under nitrogen.

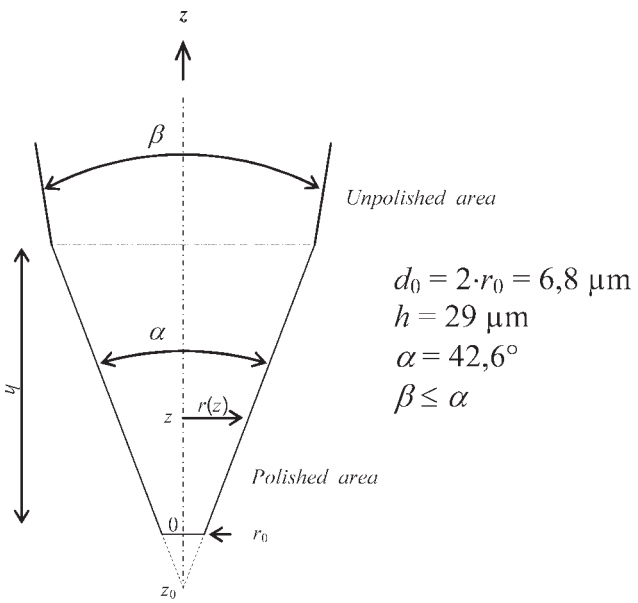

Figure 1 Flattened conical indenter geometry.

All rheometrical data obtained within 20 min were shown to be reproducible within ± 5%.

Tensile tests

The static tensile tests were carried out in a laboratory where the temperature was 23°C and the humidity was 48% according to ISO 527 using a MTS Synergie RT1000 testing apparatus. The loading speed was 1 mm min^{-1}. A MTS extensometer was used with a nominal gauge length of 25 mm. The tests were carried out at least five times for each material and the results were averaged arithmetically.

Nanoindentation measurements

Indentation tests were performed with a commercial nanoindentation system (Nanoindenter XP®, MTS Nano Instruments) at room temperature (23 ± 1°C) with a continuous stiffness measurement (CSM) technique. In this technique, an oscillating force at controlled frequency and amplitude is superimposed onto a nominal applied force. The material, which is in contact with the oscillating force, responds with a displacement phase and amplitude.[33] The hardness and elastic modulus are measured with continuous stiffness measurement and obtained from curves according to the method of Oliver and Pharr.[34] This method is described in a previous work of our team.[23]

We have used a three-side pyramid (Berkovitch) diamond indenter and a flattened conical diamond indenter; the flattened conical geometry is shown in Figure 1. For each indenter, the area function, which is used to calculate contact area Ac from contact

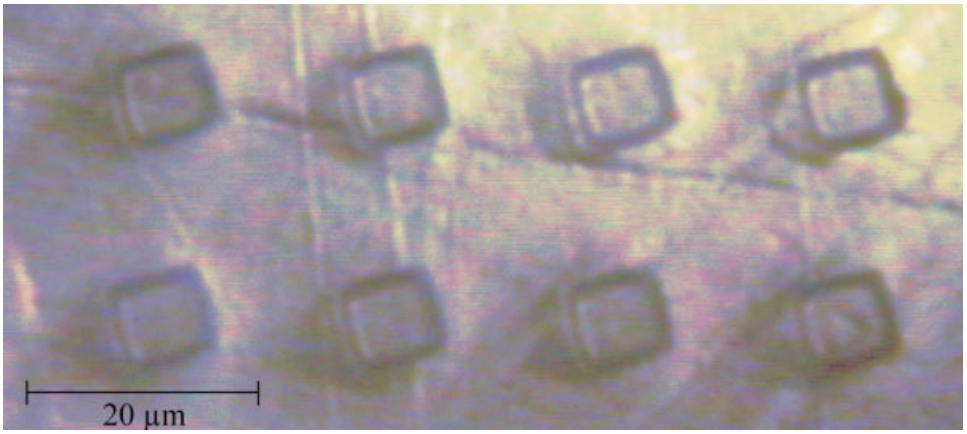

Figure 2 Indentation matrix induced by a flattened conical indenter. [Color figure can be viewed in the online issue, which is available at www.interscience.wiley.com.]

depth h_c, was carefully calibrated by using a standard sample, before the experiments.

Strain rate during loading was maintained at 0.05 s^{-1} for all the samples. We operated with a 3-nm amplitude, 70 Hz oscillation using identical load rate conditions. The Nanoindenter tests were carried out in the following sequence: first, after the indenter was made to touch the surface, it was driven into the material with constant strain rate, 0.05 s^{-1}, to a depth of 1500 nm; second, the load was held at maximum value for 60 s; and finally, the indenter was withdrawn from the surface with the same rate as loading until 10% of the maximum load was reached.

Nanoindentation experiments were performed as indents matrix. Figure 2 shows a part of an indentation matrix in one of our samples. We have been performed 10× 10 matrixes with 20 micrometers between each indent.

Only samples showing stable nanomechanical properties have been preserved in order to avoid heterogeneities into blend depth.

Thermo-Gravimetric analysis (TGA)

TGA experiments were carried out in a Setaram TG-DTA 92-10 thermal analyzer using a scanning rate of $20°C \cdot min^{-1}$ under nitrogen in the temperature range starting from 25°C to 600°C.

RESULTS AND DISCUSSION

WAXS and TEM analysis

Due to its ease and availability, WAXS is the most commonly used to probe nanocomposite structure, and the position, shape, and intensity of the different peaks may be allowed to evaluate the dispersion of mineral sheets within the polymer matrix (intercalated and/or exfoliated structures). Cloisite 30B and PLA-based nanocomposites with varying amounts of filler have been analyzed by WAXS (Fig. 3).

As expected, no peak is observed in the WAXS pattern of neat PLA between 2 and 8°, whereas the Cloisite 30B exhibits a sharp peak at around 4.8°. The d-spacing values (basal distance between clay layers) were calculated using Bragg's law ($\lambda = 2d\sin\theta$; d is the interlayer d-spacing and λ is the wave length). The d_{001} peak of Cloisite 30B appears at $2\theta = 4.8°$, corresponding to an interlayer spacing of 1.8 nm.

The PLA-based nanocomposites containing 1, 3, and 5 wt % of organoclay exhibit no significant diffraction peak in the region of $2\theta = 2$–8°, which indicates predominant, if not complete, exfoliation. However, it is noted, for the sample containing 5 wt % of Cloisite 30B, a broad peak of less intensity, which is positioned at higher angle at $2\theta \sim 5.2°$. This effect can be explained by a more heterogeneous structure of the nanocomposite, probably because of the difficulty to obtain a homogeneous material when the nanofiller content is high.[20] This result indicates the good compatibility between the organophilic clay and PLA and that the nanocomposite morphology can be considered as intercalated and/or partially exfoliated structure, whatever the filler content. Each layer of the mineral is homogeneously dispersed (or, at least, as highly intercalated structure) in the PLA matrix although a slight amount of nonexfoliated layers probably still remains, in particular for the most filled sample.

To comment these WAXS results, it is interesting to consider modeling the tensile modulus data using, for example, Hui and Shia model.[35] Taking C30B modulus as 170 GPa and its density of 2.83 g cm^{-3} [36] and PLA density of 1.25 g cm^{-3}, an apparent aspect ratio of 94 can be calculated. Considering that MMT has an aspect ratio that equals 166 ± 86,[37]

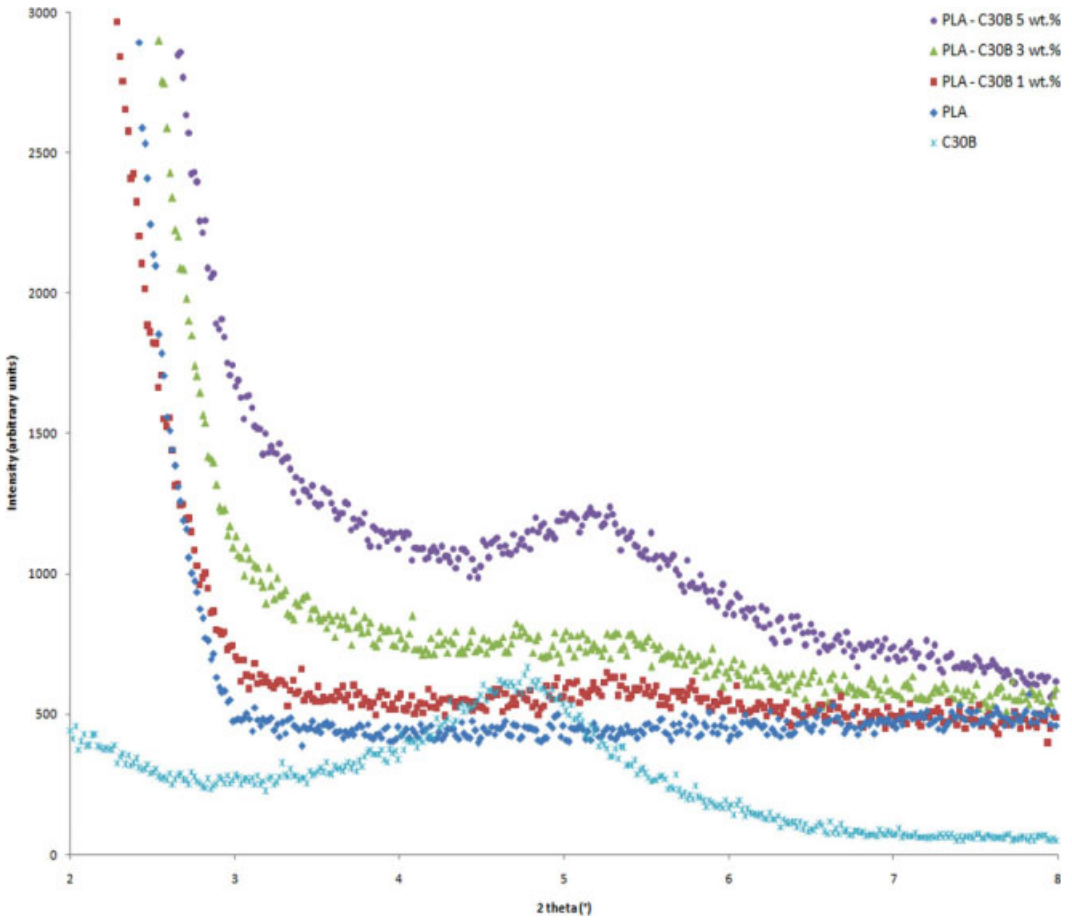

Figure 3 WAXS patterns of Cloisite 30B, neat PLA, PLA-C30B (1 wt %), PLA-C30B (3 wt %), and PLA-C30B (5 wt %) nanocomposites. [Color figure can be viewed in the online issue, which is available at www.interscience.wiley.com.]

these nanocomposites achieve a relatively good degree of exfoliation/intercalation. This highlights the fact that no large aggregates remains in the polymerized samples.

To definitively confirm the hybrid structures, the dispersion of the C30B in PLA matrix was observed by using TEM (Fig. 4).

As revealed in this image, TEM micrograph shows a nanodispersed morphology in the PLA-C30B (1 wt %) nanocomposite. On this image, the light and the dark regions represent, respectively, PLA and fillers and a heterogeneous disordered nanostructure was observed. Indeed, numerous individual clay layers coexist with a few stack of clay layers. This TEM observation suggests that at least partially exfoliated PLA-C30B nanocomposites have been obtained, in good agreement with the WAXS patterns and the theoretical model.

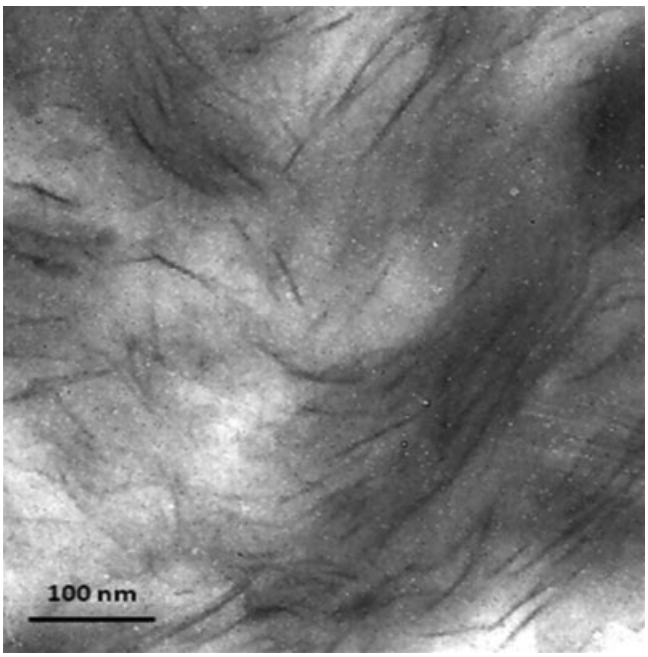

Figure 4 TEM image of the nanocomposite filled with 1 wt % of C30B.

Rheological measurements

Figure 5(a,b), show the storage modulus G′ and loss modulus G″, respectively, as a function of frequency

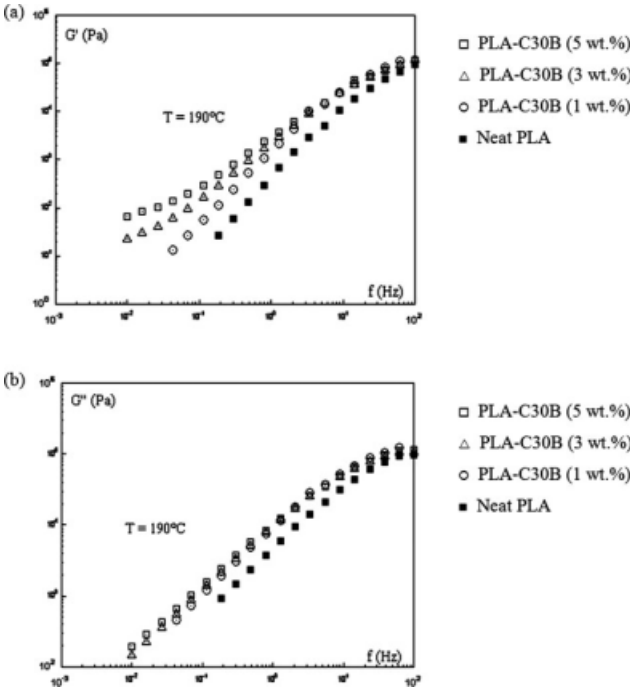

Figure 5 Viscoelastic moduli, storage modulus G′ (a) and loss modulus G″ (b), as a function of frequency, for neat PLA, PLA-C30B (1 wt %), PLA-C30B (3 wt %), and PLA-C30B (5 wt %) nanocomposites. ● PLA-C30B (5 wt %); ρ PLA-C30B (3 wt %); γ PLA-C30B (1 wt %); ν Neat PLA.

in the linear viscoelastic domain. For the PLA matrix, they indicate that in the range of accessible frequencies the terminal zone is clearly displayed, i.e. $G' \propto \omega^2$ and $G'' \propto \omega$ at lowest frequencies. Results show that, as far as the terminal zone is concerned, dynamic moduli gradually increase with clay content, the influence of clay fraction being more marked on the storage modulus. Figure 5(a) also shows that the G′ versus frequency curve exhibits a plateau in the low frequency region at silicate mass fraction above 3 wt %, meaning that the threshold mass fraction is superior to 1 wt % and inferior to 3 wt %. In fact, the storage modulus, nearly independent of frequency, is the signature of the solid-like behavior of highly filled nanocomposites on long time scales. For these structured materials (clay contents above 3 wt %), results are, qualitatively and quantitatively, in good agreement with those obtained for well-dispersed and intercalated clay/PLA nanocomposites by Ray and Okamoto.[28] However, at high frequencies, there is no significant effect of clay content: all G′ curves are close to that of the PLA matrix, suggesting that the nanocomposite structure is not completely exfoliated as suggested by TEM micrograph (Fig. 4). Indeed, a high degree of clay exfoliation leads to a significant increase of storage modulus with filler content at high frequencies.[38]

Effect of the nanofiller on tensile properties

In general, the Young's modulus (or tensile modulus), expressing the stiffness of a material at the start of a tensile test, has shown to be strongly improved when layered silicate nanofillers are homogeneously dispersed into the polymer matrix.[22] The mechanical properties of different nanocomposites based on PLA and a pure PLA sample prepared under similar conditions are summarized in Table I.

The Cloisite incorporation into PLA matrix leads to a large increase of the Young's moduli of nanocomposites at filler contents as low as a few weight percent. As seen in Table I, it is drastically increased from 3401 MPa for pure PLA to 5577 MPa for the nanocomposite containing 5 wt % of filler. The reinforcement effect R, which corresponds to the ratio of the tensile modulus of the nanocomposite to the tensile modulus of the pure polymer, can be calculated. PLA-based nanocomposites studied here yield *R* values of 1.15, 1.44, and 1.64 for 1, 3, and 5 wt %, respectively, which is significantly high. This significant enhancement in modulus by the incorporation of a small amount of organically modified clay can be attributed to a significant degree of intercalation and a non-negligible degree of exfoliation, resulting in a greater mineral-PLA matrix interfacial area.

Concerning the evolution of the maximal strength at break which expresses the ultimate strength that the material can bear before break, the differences observed are sufficiently notable to draw some comments. As seen in Table I, the tensile strength is decreased from 60.4 MPa for pure PLA to 28.8 MPa for the nanocomposite containing 5 wt % of C30B. The relationships between tensile strength, filler/matrix adhesion, and dispersion are more complex than for modulus, so no attempt is made at this time to justify the result with quantitative models.[39] Generally, tensile strength of many nanocomposites has been found to increase with increased clay content.[17] However, in nanocomposites of poly(butylene succinate)/MMT, the opposite trends has been reported.[40] In the case of thermoplastic polyurethane-based nanocomposites containing C30B, upon silicate addition large improvements in stiffness were observed,

TABLE I
Tensile Properties of Pure PLA and PLA-Based Nanocomposites Containing Various Cloisite Contents

Samples	Tensile modulus (MPa)	Tensile strength (MPa)	Elongation at break (%)
PLA	3401 ± 101	60.4 ± 0.8	4.1 ± 0.7
PLA-C30B 1 wt %	3914 ± 69	56.2 ± 1.0	3.2 ± 0.5
PLA-C30B 3 wt %	4901 ± 41	49.9 ± 1.2	1.4 ± 0.2
PLA-C30B 5 wt %	5577 ± 67	28.8 ± 2.1	0.7 ± 0.1

TABLE II
Modulus and Hardness of Pure PLA and the Different PLA-C30B Samples by Using Nanoindentation with Berkovitch or Flattened Conical Indenter

	Berkovitch indenter		Flattened conical indenter	
Samples	Modulus (MPa)	Hardness (MPa)	Modulus (MPa)	Hardness (MPa)
PLA	4360 ± 190	219 ± 18	4530 ± 60	391 ± 8
PLA-C30B 1 wt %	4380 ± 220	223 ± 22	4790 ± 40	409 ± 6
PLA-C30B 3 wt %	4970 ± 170	288 ± 19	5040 ± 80	454 ± 2
PLA-C30B 5 wt %	4990 ± 200	298 ± 22	5180 ± 70	465 ± 4

which however were accompanied by a decrease in tensile strength.[41] The reason is not clear, but it is thought that the decrease in the tensile strength is attributed to the decrease in the elongation at break, which is probably related to the delamination of the polymer-silicate interlayer.

Lastly, the elongation at break tends to decrease as expected for such materials when the interaction between the polymer and the filler becomes stronger.

Nanoindentation results

Nanoindentation measurements with Berkovitch indenter

The modulus and hardness values obtained for the different PLA samples are reported in Table II.

The values are averaged on indentation depth of 1200–1500 nm from a 10 × 10 matrix. Poisson's ratio of 0.35 was used in all modulus calculations.

In a first time, we can notice the high standard deviation values ranging from 3.5 to 10%. Good agreement is found with literature values, in particular with the results obtained by Wright-Charlesworth et al.[42] and Pillin et al.[43] (4360 compared with 4600 and 4490 MPa for neat PLA modulus). However, these values obtained by nanoindentation present an overestimation of 20% compared with modulus measured by tensile test on normalized specimens (4360 compared with 3400 MPa for neat PLA modulus). According to Rodriguez et al.,[44] we can interpret these discrepancies as an effect of a scale factor and size effect between nanoindentation and tensile tests. Another explanation of this phenomenon, suggested by Briscoe et al.,[45] could be the effect of the high hydrostatic pressure generated beneath the Berkovitch indenter.

As expected, the Table II exhibits a slight enhancement of the mechanical properties with sufficiently filled nanocomposites, but this effect is not obvious for 1 wt % of C30B. In the same way, the average modulus and hardness values of PLA reinforced with 3 and 5 wt % of C30B are quite the same.

Shen et al.[46] evidenced this phenomenon for PA 6.6-montmorillonite nanocomposites with similar clay loadings. They have shown a modest enhancement of hardness and stiffness with increasing clay concentration, elastic modulus improving by about 18% for the nanocomposite containing 5 wt % clay. This effect can be explained by a more heterogeneous structure of the nanocomposites, probably because of the difficulty to obtain a homogeneous composite at high loading rates as evidenced by WAXS results.

This heterogeneous structure of the 5 wt % clay composite could induce inaccurate nanoindentation results because of the sharp tip of the Berkovitch indenter. The penetration of the thin tip in the sample could occur in a matrix area and induce a displacement of the clay. A flattened indenter geometry like a flat punch or a flattened cone is probably more appropriate to characterize nanocomposites.

Nanoindentation measurements with flattened conical indenter

In Table II, the modulus and hardness values obtained for the different PLA samples are shown. A Poisson's ratio of 0.35 was used in all modulus calculations. The use of the flattened conical indenter shows the most progressive increase of mechanical properties with increasing clay content. It is very interesting to note that standard deviation values for modulus and hardness range from 0.4 to 2%. This decreasing into standard deviations indicates the good suitability of the flattened conical tip to the nanocomposites, the use of a flattened tip seems to be very appropriate to characterize nanocomposites.

This low scattering of the modulus values indicates a good homogeneity of our samples as also observed by rheological measurements. This phenomenon is evidenced by Figure 6 showing cartography of the calculated modulus, in the case of the nanocomposite filled with 1 wt % of C30B. This figure reveals that the modulus values are relatively constant, whatever the indent position, and the average modulus can be considered as equal to 4800 MPa. Same phenomena (figures not shown here) have been pointed out for the two other nanocomposite samples.

The hardness and modulus values obtained with the flattened conical indenter are clearly higher

(especially for the hardness) than those obtained by using the Berkovitch indenter. This phenomenon is attributed to the geometry of the indenter because of the inclination of its flanks.[47] It is expected that a uniaxial stress state allowing the calculation of a correct value for the modulus of elasticity will build up under a flat indenter body (flat punch or flat cone).

Thermogravimetric analysis (TGA)

The thermal stability of the nanocomposites has been examined by TGA at a heating rate of 20°C min^{-1} under nitrogen flow. The informations that can be considered as important to characterize thermal stability are the onset temperature which is measured both by the temperature at which 10% degradation occurs ($T_{degradation\ 10\%}$), the mid-point of the degradation ($T_{degradation\ 50\%}$) and the fraction which is not volatile at 600°C, denoted as char. The results obtained for PLA-based nanocomposites were compared with those of pure PLA. The data for pure PLA and for all the PLA-based nanocomposites are shown in Table III.

The results show that all the PLA-based nanocomposites degrade at a higher temperature than pure PLA. The thermal stability of the nanocomposites systematically increases with increasing clay content, up to a loading of 5 wt %. For example, the temperature corresponding to 10% degradation of pure PLA is 392°C, but that of the PLA-Cloisite 30B nanocomposite is 415°C, indicating a 23°C improvement with just 5 wt % of clay. Nevertheless, the compared values of $T_{degradation\ 10\%}$ and $T_{degradation\ 50\%}$ suggest that the beginning of decomposition seems to be more affected by introduction of few organoclay percents. The temperature at which 50% degradation occurs is less affected than the temperature corresponding to 10% degradation. This demonstrates that the thermal decomposition process of the material takes more time to start in the presence of few organoclay percents. When the decomposition process is initiated, the influence of the organoclay can be considered as quite negligible.

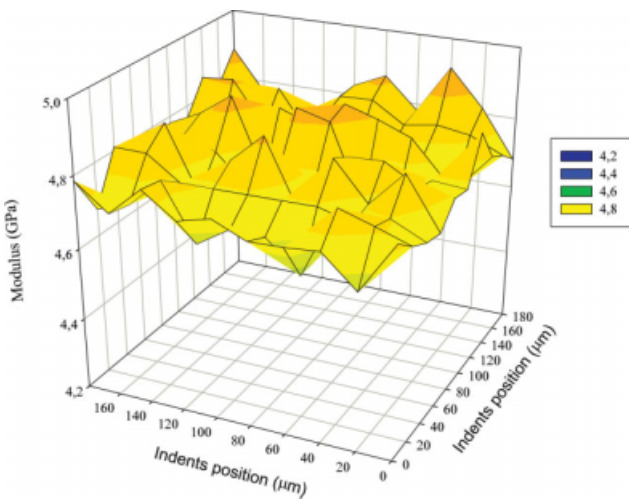

Figure 6 Cartography of the calculated modulus of the nanocomposite filled with 1 wt % of C30B. [Color figure can be viewed in the online issue, which is available at www.interscience.wiley.com.]

TABLE III
TGA Results for Pure PLA and PLA-Based Nanocomposites

Samples	$T_{degradation\ 10\%}$ (°C)	$T_{degradation\ 50\%}$ (°C)	Char at 600°C (%)
PLA	392	379	0
PLA-C30B 1 wt %	394	378	0.6
PLA-C30B 3 wt %	403	383	2.0
PLA-C30B 5 wt %	415	388	3.7

Nevertheless, it is clear that PLA nanocomposites containing few organoclay percents are more thermally stable than virgin PLA. The role of the clay in the nanocomposite structure may be the main reason for the difference in TGA results of these systems compared with pure polymer. This shift to higher temperature for the beginning of decomposition can be explained by a decrease in the diffusion of oxygen and volatile degradation products throughout composite material because of the homogeneous incorporation of clay sheets. The clay acts as a heat barrier, which enhances the overall thermal stability of the system.

CONCLUSIONS

PLA-organoclay nanocomposites have been successfully prepared by a melt intercalation method using Cloisite 30B as organoclay. The material morphology obtained from this protocol indicates that the dispersion of mineral platelets within the PLA matrix is relatively homogeneous, as revealed by WAXS, TEM and rheology. All the nanocomposites had greater thermal stability than pure PLA. As regards the mechanical behaviour of the different nanocomposites, we have shown a significant improvement in modulus and hardness with increase of clay loading, due to the addition of stiff clay nanofillers into the PLA matrix. The variations of the strength and the elongation of at break evidence a decrease with clay loading indicating an alteration of the plastic deformation of the matrix with the incorporation of clay.

Finally, this work demonstrates the good agreement between the mechanical measurements carried out using tensile tests, which can be considered as a macroscopic characterization technique, and those obtained by the nanoindentation technique which allows the determination of the mechanical properties at the nanometric scale. This good correlation of mechanical properties at the macrometric and

nanometric scales can be attributed to a high degree dispersion of nanoplatelets within the polymer matrix. However, from a quantitative point of view the increase of the modulus with the clay content is lower as probed by nanoindentation than measured by tensile test. This effect can be either due to a difference in the degree of cristallinity between the bulk and the surface of the sample or to a lower content of clay close to the surface. The highly polar character of the C30B could indeed decrease its concentration in a PLA-air interphase of at least 1500 nm. Further work will be required to better understand these slight differences between bulk and surface mechanical properties.

It can be concluded that production of an organoclay nanocomposite based on PLA can be an efficient route to extend the application of the polymer as a biodegradable material, with the possibility to finely tune properties by adjustment of the nanofiller content.

References

1. Ray, S. S.; Bousmina, M. Prog Mater Sci 2005, 50, 962.
2. Bordes, P.; Pollet, E.; Averous, L. Prog Polym Sci 2009, 34, 125.
3. Darder, M.; Aranda, P.; Ruiz-Hitzky, E. Adv Mater 2007, 19, 1309.
4. Gupta, A. P.; Kumar, V. Eur Polym J 2007, 43, 4053.
5. Lim, L. T.; Auras, R.; Rubino, M. Prog Polym Sci 2008, 33, 820.
6. Lunt, J. Polym Degrad Stab 1998, 59, 145.
7. Datta, R.; Henry, M. J Chem Technol Biotechnol 2006, 81, 1119.
8. Auras, R.; Harte, B.; Selke, S. Macromol Biosci 2004, 4, 835.
9. Garlotta, D. J Polym Environ 2001, 9, 63.
10. Weber, C. J.; Haugaard, V.; Festersen, R.; Bertelsen, G. Food Addit Contam 2002, 19, 172.
11. Okamoto, M. In Handbook of Biodegradable Polymeric Materials and Their Applications, Mallapragada, S. K., Narasimhan, B., Eds; Iowa State University: Ames, 2005.
12. Pandey, J. K.; Kumar, A. P.; Misra, M.; Mohanty, A. K.; Drzal, L. T.; Singh, R. P. J Nanosci Nanotech 2005, 5, 497.
13. Krikorian, V.; Pochan, D. J. Chem Mater 2003, 15, 4317.
14. Pluta, M.; Galeski, A.; Alexandre, M.; Paul, M. A.; Dubois, P. J Appl Polym Sci 2002, 86, 1497.
15. Ray, S. S.; Yamada, K.; Okamoto, M.; Ueda, K. Nano Lett 2002, 2, 1093.
16. Ray, S. S.; Okamoto, M. Macromol Rapid Commun 2003, 24, 815.
17. Ray, S. S.; Okamoto, M. Prog Polym Sci 2003, 28, 1539.
18. Bruzaud, S.; Levesque, G. Chem Mater 2002, 14, 2421.
19. Beigbeder, A.; Bruzaud, S.; Médéric, P.; Aubry, T.; Grohens, Y. Polymer 2005, 46, 12279.
20. Bruzaud, S.; Grohens, Y.; Ilinca, S.; Carpentier, J. F. Macromol Mater Eng 2005, 290, 1106.
21. Lebrun, L.; Bruzaud, S.; Grohens, Y.; Langevin, D. Eur Polym J 2006, 42, 1975.
22. Bruzaud, S.; Carpentier, J. F.; Grohens, Y. Macromol Mater Eng 2004, 289, 531.
23. Bruzaud, S.; Bourmaud, A. Polym Test 2007, 26, 652.
24. Touati, N.; Kaci, M.; Ahouari, H.; Bruzaud, S.; Grohens, Y. Macromol Mater Eng 2007, 292, 1271.
25. Remili, C.; Kaci, M.; Kachbi, S.; Bruzaud, S.; Grohens, Y. J Appl Polym Sci 2009, 112, 2868.
26. Krishnamoorti, R.; Yurekli, K. Curr Opin Colloid Interface Sci 2001, 6, 464.
27. Aubry, T.; Razafinimaro, T.; Médéric, P. J Rheol 2005, 49, 425.
28. Ray, S. S.; Okamoto, M. Macromol Mater Eng 2003, 288, 936.
29. Peng, H.; Tjiu, W. C.; Shen, L.; Huang, S.; He, C.; Liu, T. Comp Sci Technol 2009, 69, 991.
30. Lam, C. K.; Lau, K. T. Comp Struct 2006, 75, 553.
31. Wong, S. C.; Lee, H.; Qu, S.; Mall, S.; Chen, L. Polymer 2006, 47, 7477.
32. Mammeri, F.; Le Bourhis, E.; Rozes, L.; Sanchez, C. J Eur Ceram Soc 2006, 26, 259.
33. Li, X.; Bhushan, B. Mater Charact 2002, 48, 11.
34. Oliver, W. C.; Pharr, G. M. J Mater Res 1992, 7, 1564.
35. Hui, C. Y.; Shia, D. Polym Eng Sci 1998, 38, 774.
36. Fornes, T. D.; Paul, D. R. Polymer 2003, 44, 4993.
37. Ploehn, H. J.; Liu, C. Ind Eng Chem Res 2006, 45, 7025.
38. Lim, Y. T.; Park, O. O. Rheol Acta 2001, 40, 220.
39. Stretz, H. A.; Paul, D. R.; Li, R.; Keskkula, H.; Cassidy, P. E. Polymer 2005, 46, 2621.
40. Someya, Y.; Nakazato, T.; Teramoto, N.; Shibata, M. J Appl Polym Sci 2004, 91, 1463.
41. Finnigan, B.; Martin, D.; Halley, P.; Truss, R.; Campbell, K. Polymer 2004, 45, 2249.
42. Wright-Charlesworth, D. D.; Miller, D. M.; Miskioglu, I.; King, J. A. J Biomed Mater Res Part A 2005, 74, 388.
43. Pillin, I.; Montrelay, N.; Bourmaud, A.; Grohens, Y. Polym Degrad Stab 2008, 93, 321.
44. Rodríguez, R.; Gutierrez, I. Mater Sci Eng A 2003, 361, 377.
45. Briscoe, B. J.; Sebastian, K. S. Proc R Soc London 1996, 452, 439.
46. Shen, L.; Phang, I. Y.; Chen, L.; Liu, T.; Zeng, K. Polymer 2004, 45, 3341.
47. Gindl, W.; Reifferscheid, M.; Adusumalli, R. B.; Weber, H.; Röder, T.; Sixta, H.; Schöberl, T. Polymer 2008, 49, 792.